2017 21st International Conference on Process Control (PC)
June 6–9, 2017, Štrbské Pleso, Slovakia

# Identification of n-link Inverted Pendulum on a Cart

Jana Königsmarková, Miloš Schlegel
NTIS - New Technologies for the Information Society, Faculty of Applied Sciences, University of West Bohemia,
Technická 8, Pilsen, Czech Republic, Email: jkonig@kky.zcu.cz, schlegel@kky.zcu.cz

*Abstract*—**The identification procedure specially designed for an n-link inverted pendulum on a cart is presented. By the Lagrangian mechanics, the mathematical model of the n-link inverted pendulum is established initially. To fully model the system, the standard dynamic parameters which are some algebraic functions of geometric, inertial, and friction parameters are introduced. Because the dynamic model of the n-link inverted pendulum is linear with respect to these parameters, the ordinary and weighted least squares techniques can be applied to estimation their values and the corresponding standard deviations. Also, the exact algorithms for numerical differentiation used in the formation of the regression model are described in detail. Finally, the results from identification of the real triple inverted pendulum are presented.**

## I. Introduction

Since around 1960, the inverted pendulum on a cart is a very popular physical model living in control laboratories to verify some control theory or method in automatic control domain. The main reason for this is that it constitutes an underactuated system with a nonlinear, unstable and nonminimum-phase behavior and thus reveals many interesting system-theoretic properties. The stabilization in the upper position task and swing-up problem, where the pendulum is moved from the lower to the upper pendulum configuration, has attracted much attention [1]–[4]. Both these problems are relatively easy for a simple pendulum, but become significantly more complex for a double, triple, or even n-link inverted pendulum (nLIP), $n > 3$. Most advanced control schemes formulated in the recent literature for the nLIP require dynamic models. The model precision must rapidly grow with the multiplicity of the pendulum. For a triple pendulum model based stabilization control, it is needed to know at least the eight model parameters with an accuracy of about three significant decimal digits, even in the case of a mere simulation experiment.

Model formulation in terms of equations, in the case of the nLIP with viscous friction, is a well-studied subject. For example, Lagrange formalism can be used [5]. Besides model equations, dynamic model parameters must also be determined. These parameters are constant and must be identified to fully model the pendulum. There are three main methods, applicable to the nLIP, for estimating dynamic model parameters:

(i) Physical experiments with the isolated links (determination of the link mass, center-of-mass, and inertia tensor). This method is very tedious and should be realized before assembling the pendulum. Note, that this method was used in a recent paper [1] to identify the parameters of a triple inverted pendulum.

(ii) Using CAD/CAM to calculate the geometric and inertia parameters from 3D models. This method is prone to errors due to the fact that the geometry of the links is complicated to define precisely, and that certain parts such as bearing, bolts nuts, and washers are generally neglected.

(iii) Identification based on the input/output behavior of the system on some motion trajectory and on estimating the parameter values by minimizing the difference between a function of the real system variables and its mathematical model. This method was found to be the best in terms of ease of experimentation and precision of the obtained values in the field of robotics [5].

In recent decades, the identification based on the input/output behavior was widely used to enhance the performance of robots. The dynamic model of a robot relates the full motion of its joints - positions, velocities and accelerations - with the forces or torques being applied to those joints. For the purposes of control of an inverted pendulum on a card it is more convenient to consider the cart accelerations as the input instead the force acting on the cart. Moreover, the inverted pendulums are underactuated systems with passive joints. For these reasons, it is necessary to modify the existing identification procedure considerably. This paper focuses on this task.

Now, we shortly describe the principle of the identification procedure developed in this paper. Although being composed by large expressions, the nLIP dynamic model is linear with respect to some dynamic parameters, which are some algebraic functions of geometric, inertial, and friction parameters (from now on called physical parameters) of pendulum links. The dynamic parameters can be classified into three groups: fully identifiable, identifiable in linear combination, and completely unidentifiable. In order to obtain a unique solution, we have to introduce some identifiable parameters, which are called bellow *standard dynamic parameters*. Note, that the concept of identifiable parameters was originally introduced in connection with the identification of dynamic models of robots [5]. It is noteworthy that we cannot determine all physical parameters of the nLIP, from any set of identifiable parameters. On the other hand, standard dynamic parameters uniquely define the dynamic behavior of the system. The set of standard dynamic parameters can be estimated by the least square solution of an overdetermined linear system of equations called a regression model. The regression model is obtained by a time equidistant sampling of dynamic model along a proper trajectory. Therefore, the data matrices of the regression model

978-1-5386-4011-1/17/$31.00  

are created from the measured angles of the revolute joints of the nLIP, its first and second derivatives, and the acceleration of the cart.

This paper is concerned with the design and experimental validation of the identification procedure specially designed for the nLIP. The developed procedure was used to obtain a model of a real triple inverted pendulum. The resulting model was successfully used to solve both the problem of swing-up and stabilization in the upper position. A video that demonstrates this fact can be found at https://www.youtube.com/watch?v=SWupnDzynNU, for more details see [6].

## II. Dynamical equations of the model in the parameters identifiable in linear combination

Let us derive the dynamical equations of motion of the n-link inverted pendulum on a cart using the Lagrange method. The coordinates in the Euler-Lagrange equations are: $y_0$ position of a cart, $\delta_i$, $i = 1, \ldots, n$, angle of $i$-th link, with respect to the vertical axis. Each link of pendulum is characterized by its five physical parameters: the link mass $m_i$, the link length $l_i$, the relative position $a_i$ of center of gravity, i.e. $|A_{i-1}T_i| = a_i l_i$, where $T_i$ is the center of gravity of the $i$-th link, $A_i$ denotes the $i$-th revolute joint (see Fig. 1), $J_i$ denotes the moment of inertia about the axis through the center of gravity, and $b_i$ denotes the coefficient of fluid friction in the $i$-th joint, thus the total number of these parameters is $5n$. Unfortunately, these parameters can not be directly identifiable. In this section we show, that for arbitrary $n$, we can introduce the vector of the standard dynamic parameters $\theta$, which are directly identifiable.

Consider the notations introduced in Fig. 1, and denote the y-coordinate of the point $T_i$ as $Y_i$, and its z-coordinate as $Z_i$, $\imath = 1, 2, \ldots, n$. Now, it follows

$$Y_i = \sum_{j=1}^{i} l_j \sin\delta_j + a_i l_i \sin\delta_i + y_0$$

$$Z_i = \sum_{j=1}^{i} l_j \cos\delta_j + a_i l_i \cos\delta_i.$$

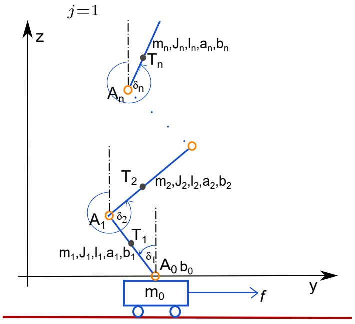


Figure 1. Model of $n-$link inverted pendulum on a cart.

For potential energy $V$ and kinetic energy $T$ of the nLIP we obtain

$$V = \sum_{k=1}^{n} m_k g Z_k$$

$$T = \sum_{k=1}^{n} \frac{1}{2}\left\{ m_k \left[ \left(\frac{\mathrm{d}Y_k}{\mathrm{d}t}\right)^2 + \left(\frac{\mathrm{d}Z_k}{\mathrm{d}t}\right)^2 \right] \right\} + \frac{1}{2} m_0 \left(\frac{\mathrm{d}y_0}{\mathrm{d}t}\right)^2. \tag{1}$$

Equations (1) lead for arbitrary $n$ to

$$V_n = \sum_{i=1}^{n} m_i g \left( \sum_{j=1}^{i-1} l_j \cos\delta_j + a_i l_i \cos\delta_i \right) \tag{2}$$

$$T_n = \sum_{k=1}^{n} \left[ \frac{1}{2} \sum_{i=1}^{k-1} m_k l_i^2 \dot\delta_i^2 + \sum_{j=1, j>i}^{k-1} \sum_{i=1}^{k-1} m_k l_i l_j \dot\delta_1 \dot\delta_j \cos(\delta_i - \delta_j) + \right.$$
$$\sum_{j=1}^{k-1} m_k a_k l_j l_k \dot\delta_j \dot\delta_k \cos(\delta_j - \delta_k) + \sum_{j=1}^{k-1} m_k l_j \dot\delta_j \dot y_0 \cos\delta_j + \frac{1}{2} m_k \dot y_0^2 +$$
$$\left. + \frac{1}{2} m_k a_k^2 l_k^2 \dot\delta_k^2 + m_k a_k l_k \dot\delta_k \dot y_0 \cos\delta_k + \frac{1}{2} J_k \dot\delta_k \right] + \frac{1}{2} m_0 \dot y_0^2. \tag{3}$$

*Proposition 1:* For arbitrary $n$, the potential energy of the $n-$link inverted pendulum on a cart can be expressed as

$$V_n = \sum_{i=1}^{n} \nu_i g \cos\delta_i, \tag{4}$$

$$\text{where} \quad \nu_i = m_i a_i l_i + l_i \left( \sum_{j=i+1}^{n} m_j \right), \qquad i = 1, \ldots, n. \tag{5}$$

*Proposition 2:* For arbitrary $n$, the kinetic energy of the $n-$link inverted pendulum on a cart can be expressed as

$$T_n = \frac{1}{2} \sum_{i=1}^{n} \kappa_i \dot\delta_i^2 + \sum_{j=2, j>i}^{n} \sum_{i=1}^{n-1} \mu_{ij} \dot\delta_i \dot\delta_j \cos(\delta_i - \delta_j) +$$
$$+ \sum_{i=1}^{n} \nu_i \dot\delta_i \dot y_0 \cos\delta_i + \frac{1}{2} \dot y_0^2 \sum_{i=0}^{n} m_i, \tag{6}$$

$$\text{where} \quad \kappa_i = J_i + m_i a_i^2 l_i^2 + l_i^2 \sum_{k=i+1}^{n} m_k, \qquad i = 1, \ldots, n \tag{7}$$

$$\mu_{ij} = l_i (m_j a_j l_j + l_j \sum_{k=j+1}^{n} m_k), 2 \le j \le n, 1 \le i \le n-1, i < j.$$

**Proof.** The Propositions 1 and 2 can be simply proven by the mathematical induction. □

Moreover, the Rayleigh's dissipation function is given by

$$D = \frac{1}{2} b_1 \dot\delta_1^2 + \sum_{k=2}^{n} \frac{1}{2} b_k \left( \dot\delta_k - \dot\delta_{k-1} \right)^2 + \frac{1}{2} b_0 \dot y_0^2, \tag{8}$$

where $b_i$, for $i = 0, \ldots, n$ denotes the friction coefficient in the $i$-th joint.

If we define $q_i = \delta_i$, $i = 1, \ldots, n$, $q_{n+1} = y_0$, $\dot q_0 = 0$, and $f$ denotes the external force on the cart, then for $L = T - V$ it follows

$$0 = \frac{\mathrm{d}}{\mathrm{d}t} \frac{\partial L}{\partial \dot q_i} - \frac{\partial L}{\partial q_i} + \frac{\partial D}{\partial \dot q_i} = \kappa_i \ddot q_i + \sum_{j=1, j\neq i}^{n} \mu_{ij} \ddot q_j \cos(q_i - q_j) +$$
$$+ \sum_{j=1, j\neq i}^{n} \mu_{ij} \dot q_j^2 \sin(q_i - q_j) + \nu_i \cos q_i \ddot q_{n+1} - \nu_i g \sin q_1 +$$
$$+ b_i (\dot q_i - \dot q_{i-1}) - b_{i+1} (\dot q_{i+1} - \dot q_i), \tag{9}$$

$$f = \frac{\mathrm{d}}{\mathrm{d}t} \frac{\partial L}{\partial \dot q_{n+1}} - \frac{\partial L}{\partial q_{n+1}} + \frac{\partial D}{\partial \dot q_{n+1}} =$$
$$= \sum_{i=1}^{n} \nu_i \ddot q_j \cos(q_i) - \sum_{i=1}^{n} \nu_i \dot q_i^2 \sin q_i + \ddot q_{n+1} \left( \sum_{i=0}^{n} m_i \right) + b_0 \ddot q_{n+1}.$$

Because, with respect to $y_0$, equation (9) depends only on its second derivative $\ddot{y}_0$, we can consider that the cart acceleration represents the input $u$ of the nLIP, i.e. $\ddot{y}_0 = u$. The equation for $y_0$ can be completely omitted in this case. By reordering the terms in (9) we obtain the matrix model

$$M(q)\ddot{q} + C(q,\dot{q})\dot{q} + G(q)q = V(q)u, \tag{10}$$

where $q$ is the $n$-th vector of the joint angles and the matrices $M(q), C(q,\dot{q}), G(q), V(q)$ are given by (11).
The dynamic model (10) is linear in the $r$-vector

$$\tilde{\theta} = [\mu_{12}, \mu_{13}, \ldots, \mu_{1n}, \mu_{23}, \ldots, \mu_{2n}, \ldots, \mu_{n-1n}, \\ \kappa_1, \ldots, \kappa_n, \nu_1, \ldots, \nu_n, b_1, \ldots, b_n]^T, \tag{12}$$

containing the parameters introduced in the Propositions 1, 2, and in the equation (8). Thus, (10) can be expressed in the form

$$\tilde{\Phi}(q,\dot{q},\ddot{q},u)\tilde{\theta} = 0, \tag{13}$$

where $\tilde{\Phi}(q,\dot{q},\ddot{q},u) = \left[\,\tilde{\Phi}_1\ \tilde{\Phi}_2\ \tilde{\Phi}_3\ \tilde{\Phi}_4\right]$ is $n \times r$ matrix, depending on the joint angles $q$, velocities $\dot{q}$, accelerations $\ddot{q}$ and the acceleration $u$ of the cart and

$$\tilde{\Phi}_1 = \left[\begin{array}{cccc|cccc|c|c} f_{1,2} & f_{1,3} & \cdots & f_{1,n} & 0 & \cdots & \cdots & 0 & \cdots & 0 \\ f_{2,1} & 0 & \cdots & 0 & f_{2,3} & f_{2,4} & \cdots & f_{2,n} & \cdots & 0 \\ & & & & & & & & & \\ 0 & f_{3,1} & & & f_{3,2} & 0 & \cdots & 0 & \cdots & \vdots \\ \vdots & & \ddots & & & \ddots & & & \cdots & f_{n-1,n} \\ 0 & & & f_{n,1} & 0 & & & f_{n,2} & \cdots & f_{n,n-1} \end{array}\right],$$

$$\tilde{\Phi}_2 = \text{diag}\left(g_1, \ldots, g_n\right), \tilde{\Phi}_3 = \text{diag}\left(h_1, \ldots, h_n\right),$$

$$\tilde{\Phi}_4 = \begin{bmatrix} k_1 & -k_{1,2} & 0 & \cdots & 0 \\ 0 & k_{1,2} & -k_{2,3} & & \\ \vdots & 0 & k_{2,3} & \ddots & \\ \vdots & & \ddots & \ddots & -k_{n-1\,n} \\ 0 & & & 0 & k_{n-1\,n} \end{bmatrix},$$

$f_{i,j} \triangleq f(q_i, q_j) = \cos(q_i - q_j)\ddot{q}_j + \sin(q_i - q_j)\dot{q}_j^2$, for $i, j = 1, \ldots, n$, $i \neq j$, $g_i = \ddot{q}_i$, $h_i = u\cos q_i - g\sin q_i$, for $i = 1, \ldots, n$, $k_1 = \dot{q}_1$ and $k_{i,j} = \dot{q}_j - \dot{q}_i$, for $i = 1, \ldots, n-1$, $j = i + 1$.

Now, we divide each equation of the system (13) by $\mu_{n-1\,n}$. So, we obtain the new system of equations in the form

$$\Phi(q,\dot{q},\ddot{q},u)\theta = \Psi(q,\dot{q},\ddot{q},u), \tag{14}$$

The equation (14) represents the regression model, where $\Phi(q,\dot{q},\ddot{q},u)$ is $n \times (r-1)$ matrix, $\theta$ is $(r-1)$- vector of parameters, and $\tilde{\Phi}(q,\dot{q},\ddot{q},u)$ is $n$-vector, and all these symbols are given by (15), the dimension $(r-1)$ of the vector $\theta$ is equal to $3n + \frac{n(n-1)}{2} - 1$. Tab. II presents the explicit form of the standard dynamic parameters.

## III. Estimation of the pendulum parameters

Pendulum identification deals with the problem of estimating the model parameters $\theta$ from the data measured during a pendulum excitation experiment. The data are sequences of joint angles and cart positions from which a sequence of joint velocities and accelerations are calculated by a numerical differentiation.

### A. Numerical differentiation

The classical approach of computing derivative numerically relies on central differences derived from polynomial interpolations. Since such interpolation lacks for high-frequencies suppression, they work well only for noiseless functions whose values can be computed precisely. In the case of noisy function/data central differences give inadequate results. To resolve this problem Lanczos differentiators (Savitzky-Golay filters) use smoothing least-squares polynomial approximation to remove noise from the data. Such methods are much more robust to noise, however due to least-squares nature Lanczos differentiators cannot guarantee complete noise suppression at high frequencies. For these reasons the method of noise-robust numerical differentiation [7] based on Padé like approximation in the frequency domain is applied here. The method requires fulfillment of the following requirements: exactness on polynomials, preciseness on low frequencies and noise suppression at high frequencies. The first derivative noise - robust filter can be written in general form as

$$f'(x_0) \approx \frac{1}{h}\sum_{k=1}^{M} c_k(f_k - f_{-k}), \tag{16}$$

where $M = (N-1)/2$, $N$ is an odd integer denoting the filter length, $f_k$, $k = -M, \ldots, M$ are function values sampled at $N$ equidistant points around $x_0$ with some step $h$, and $c_k$, $k = 1, \ldots, M$, denote the filter coefficients. The frequency response of the filter (16) for $h = 1$ can be expressed in the form

$$H(\omega) = 2j\sum_{k=1}^{M} c_k \sin(k\omega).$$

The filter coefficients $c_k$, $k = 1, \ldots, M$, are determined in such way that $H(\omega)$ will be as close as possible to the frequency response of an ideal differentiator $H_d(\omega) = j\omega$ in low frequency region and smoothly tend to zero towards the highest frequency $\omega = \pi$. These requirements can be expressed well by the following linear equations

$$\left.\frac{\partial^i H(\omega)}{\partial\omega^i}\right|_{\omega=0} = \left.\frac{\partial^i H_d(\omega)}{\partial\omega^i}\right|_{\omega=0}, i = 0, \ldots, m_0, \\ \left.\frac{\partial^l H(\omega)}{\partial\omega^l}\right|_{\omega=\pi} = 0, l = 0, \ldots, m, \tag{17}$$

where the integers $m_0$ and $m$ are selected in such way that (17) has a unique solution for unknown coefficients $c_k, k = 1, \ldots, M$. If we select $m_0 = 2$ and $m = (N-3)/2$, then the solution of (17) is given by

$$c_k = \frac{1}{2^{2m+1}}\left[\begin{pmatrix} 2m \\ m-k+1 \end{pmatrix} - \begin{pmatrix} 2m \\ m-k-1 \end{pmatrix}\right], k = 1, \ldots, M. \tag{18}$$

In the pendulum identification, the velocities are computed by the filter (16), where $N = 51$ and $h = 0.001[s]$. The corresponding frequency response of the applied filter is shown in Fig. 2. The second derivative noise-robust filter is given by the formula

$$f''(x_0) \approx \frac{1}{2^{N-3}h^2}\left(s_0 f_0 + \sum_{k=1}^{M} s_k(f_k + f_{-k})\right), \tag{19}$$

$$M(q)=\begin{bmatrix} \kappa_1 & \mu_{12}\cos(q_1-q_2) & \mu_{13}\cos(q_1-q_3) & \cdots & \cdots & \mu_{1n}\cos(q_1-q_n) & 0 \\ \mu_{12}\cos(q_1-q_2) & \kappa_2 & \mu_{23}\cos(q_2-q_3) & \cdots & \cdots & \mu_{2n}\cos(q_2-q_n) & 0 \\ \mu_{13}\cos(q_1-q_3) & \mu_{23}\cos(q_2-q_3) & \kappa_3 & \ddots & \ddots & \mu_{3n}\cos(q_3-q_n) & 0 \\ \vdots & \ddots & \ddots & \ddots & \ddots & \vdots & \vdots \\ \vdots & \ddots & \ddots & \ddots & \kappa_{n-1} & \mu_{n-1\,n}\cos(q_{n-1}-q_n) & 0 \\ \mu_{1n}\cos(q_1-q_n) & \cdots & \cdots & \cdots & \mu_{n-1\,n}\cos(q_{n-1}-q_n) & \kappa_n & 0 \\ 0 & \cdots & \cdots & \cdots & \cdots & 0 & 1 \end{bmatrix}$$

$$C(q,\dot{q})=\begin{bmatrix} b_1+b_2 & \text{-}b_2+\mu_{12}\dot{q}_2\sin(q_1\text{-}q_2) & \mu_{13}\dot{q}_3\sin(q_1\text{-}q_3) & \cdots & \mu_{1n}\dot{q}_n\sin(q_1\text{-}q_n) & 0 \\ \text{-}b_2\text{-}\mu_{12}\dot{q}_1\sin(q_1\text{-}q_2) & b_2+b_3 & \text{-}b_3+\mu_{23}\dot{q}_3\sin(q_2\text{-}q_3) & \cdots & \mu_{2n}\dot{q}_n\sin(q_2\text{-}q_n) & \vdots \\ \text{-}\mu_{13}\dot{q}_1\sin(q_1\text{-}q_3) & \text{-}b_3\text{-}\mu_{13}\dot{q}_1\sin(q_1\text{-}q_3) & \ddots & \ddots & \dot{q}_n\vdots & \vdots \\ \vdots & \ddots & \ddots & \ddots & \vdots & \vdots \\ \vdots & \ddots & \ddots & b_{n\text{-}1}+b_n & \text{-}b_n+\mu_{n\text{-}1\,n}\dot{q}_n\sin(q_{n\text{-}1}\text{-}q_n) & 0 \\ \text{-}\mu_{1n}\dot{q}_1\sin(q_1\text{-}q_n) & \cdots & \cdots & \text{-}b_n\text{-}\mu_{n\text{-}1\,n}\dot{q}_{n\text{-}1}\sin(q_{n\text{-}1}\text{-}q_n) & b_n & 0 \\ 0 & \cdots & \cdots & \cdots & 0 & 0 \end{bmatrix}$$

$$G(q)=\operatorname{diag}\left(\frac{-\nu_1 g\sin q_1}{q_1},\frac{-\nu_2 g\sin q_2}{q_2},\ldots,\frac{-\nu_n g\sin q_n}{q_n},0\right),\quad V=\begin{bmatrix} -\nu_1\cos q_1 & -\nu_2\cos q_2 & \ldots & -\nu_n\cos q_n & 1 \end{bmatrix}^T. \tag{11}$$

$$\Phi(q,\dot{q},\ddot{q},u)=\left[\begin{array}{ccccc|ccccc|c|cc|cccc|cccc|ccccc} f_{1,2} & f_{1,3} & \cdots & \cdots & f_{1,n} & 0 & \cdots & \cdots & \cdots & 0 & \cdots & 0 & 0 & g_1 & 0 & \cdots & 0 & h_1 & 0 & \cdots & 0 & k_1 & \text{-}k_{12} & 0 & \cdots & 0 \\ f_{2,1} & 0 & \cdots & \cdots & 0 & f_{2,3} & f_{2,4} & \cdots & \cdots & f_{2,n} & \cdots & 0 & 0 & 0 & g_2 & & & 0 & h_2 & & & 0 & k_{12} & \text{-}k_{23} & & \\ 0 & f_{3,1} & & & & f_{3,2} & 0 & \cdots & & 0 & \cdots & \vdots & \vdots & \vdots & & & & \vdots & & & & & & & & \\ \vdots & & \ddots & & & & & \ddots & & & \cdots & f_{n-2,n-1} & f_{n-2,n} & & & \ddots & & & & \ddots & & \vdots & & \ddots & \ddots & \\ 0 & & & f_{n-1,1} & & 0 & & & f_{n-1,2} & & \cdots & f_{n-1,n-2} & 0 & \vdots & & & & \vdots & & & & & & & & \text{-}k_{n\text{-}1\,n} \\ 0 & & & & f_{n,1} & 0 & & & & f_{n,2} & \cdots & 0 & f_{n,n-2} & 0 & & & g_n & 0 & & & h_n & 0 & & & & k_{n\text{-}1\,n} \end{array}\right],$$

$$\theta=\Big[\ \frac{\mu_{12}}{\mu_{n-1\,n}}\quad \frac{\mu_{13}}{\mu_{n-1\,n}}\quad \cdots\quad \frac{\mu_{1n}}{\mu_{n-1\,n}}\quad \frac{\mu_{23}}{\mu_{n-1\,n}}\quad \cdots\quad \frac{\mu_{2n}}{\mu_{n-1\,n}}\quad \cdots\quad \frac{\mu_{n-2\,n-1}}{\mu_{n-1\,n}}\quad \frac{\mu_{n-2\,n}}{\mu_{n-1\,n}}$$

$$\frac{\kappa_1}{\mu_{n-1\,n}}\quad \cdots\quad \frac{\kappa_n}{\mu_{n-1\,n}}\quad \frac{\nu_1}{\mu_{n-1\,n}}\quad \cdots\quad \frac{\nu_n}{\mu_{n-1\,n}}\quad \frac{b_1}{\mu_{n-1\,n}}\quad \cdots\quad \frac{b_n}{\mu_{n-1\,n}}\ \Big]^T$$

$$\Psi(q,\dot{q},\ddot{q},u)=\begin{bmatrix} 0 & 0 & 0 & \ldots & 0 & -f_{n-1,n} & -f_{n,n-1} \end{bmatrix}^T. \tag{15}$$

Table I
EXPLICIT FORMULAS OF THE STANDARD DYNAMIC PARAMETERS FOR SIMPLE, 2−LINK, 3−LINK, AND 4−LINK PENDULUM.

| $n$ | Standard dynamic parameters $\left(\frac{\mu_{12}}{\mu_{n-1\,n}},\ldots,\frac{\mu_{n-2\,n}}{\mu_{n-1\,n}},\frac{\kappa_1}{\mu_{n-1\,n}},\ldots,\frac{\kappa_n}{\mu_{n-1\,n}},\frac{\nu_1}{\mu_{n-1\,n}},\ldots,\frac{\nu_n}{\mu_{n-1\,n}},\frac{b_1}{\mu_{n-1\,n}},\ldots,\frac{b_n}{\mu_{n-1\,n}}\right)$ |
|---|---|
| 1 | $\frac{J_1+m_1a_1^2l_1^2}{m_1a_1l_1}$ $\frac{b_1}{m_1a_1l_1}$ |
| 2 | $\frac{\left(m_1{a_1}^2+m_2\right){l_1}^2+J_1}{m_2a_2l_2l_1}$ $\frac{{a_2}^2{l_2}^2m_2+J_2}{m_2a_2l_2l_1}$ $\frac{m_1a_1+m_2}{m_2a_2l_2}$ $\frac{1}{l_1}$ $\frac{b_1}{m_2a_2l_2l_1}$ $\frac{b_2}{m_2a_2l_2l_1}$ |
| 3 | $\frac{l_1(m_2a_2+m_3)}{a_3l_3m_3}$ $\frac{l_1}{l_2}$ $\frac{\left(m_1{a_1}^2+m_2+m_3\right){l_1}^2+J_1}{a_3l_3m_3l_2}$ $\frac{\left(m_2{a_2}^2+m_3\right){l_2}^2+J_2}{a_3l_3m_3l_2}$ $\frac{{a_3}^2{l_3}^2m_3+J_3}{a_3l_3m_3l_2}$<br>$\frac{l_1(m_1a_1+m_2+m_3)}{a_3l_3m_3l_2}$ $\frac{a_2m_2+m_3}{a_3l_3m_3}$ $\frac{1}{l_2}$ $\frac{b_1}{a_3l_3m_3l_2}$ $\frac{b_2}{a_3l_3m_3l_2}$ $\frac{b_3}{a_3l_3m_3l_2}$ |
| 4 | $\frac{l_1l_2(a_2m_2+m_3+m_4)}{m_4a_4l_4l_3}$ $\frac{l_1(a_3m_3+m_4)}{m_4a_4l_4}$ $\frac{l_2(a_3m_3+m_4)}{m_4a_4l_4}$ $\frac{l_1}{l_3}$<br>$\frac{l_2}{l_3}$ $\frac{\left(m_1{a_1}^2+m_2+m_3+m_4\right){l_1}^2+J_1}{m_4a_4l_4l_3}$ $\frac{\left({a_2}^2m_2+m_3+m_4\right){l_2}^2+J_2}{m_4a_4l_4l_3}$ $\frac{\left({a_3}^2m_3+m_4\right){l_3}^2+J_3}{m_4a_4l_4l_3}$<br>$\frac{{a_4}^2{l_4}^2m_4+J_4}{m_4a_4l_4l_3}$ $\frac{l_1(m_1a_1+m_2+m_3+m_4)}{m_4a_4l_4l_3}$ $\frac{l_2(a_2m_2+m_3+m_4)}{m_4a_4l_4l_3}$ $\frac{a_3m_3+m_4}{m_4a_4l_4}$<br>$\frac{l_1}{l_3}$ $\frac{b_1}{m_4a_4l_4l_3}$ $\frac{b_2}{m_4a_4l_4l_3}$ $\frac{b_3}{m_4a_4l_4l_3}$ $\frac{b_4}{m_4a_4l_4l_3}$ |

where $N \geq 5$ is an odd integer denoting the filter length, and $M = (N-1)/2$. The coefficients $s_k, k = 0,\ldots,M$, are calculated for any $N$ by simple recursive Algorithm 1.

In the pendulum identification, the accelerations are computed by the filter (19), where $N = 101$ and $h = 0.001[s]$. The corresponding frequency response of the applied filter is shown in Fig. 3.

*B. Least square estimation*

From a time equidistant sampling of dynamical model (15) along a trajectory $(q, \dot{q}, \ddot{q}, u)$, we obtain the overdetermined

| *Algorithm* 1: Calculation of $s_k$, $k = M, \ldots, 0$ |
|---|
| if $k > M$ then return 0; |
| if $k = M$ then return 1; |
| return $[(2N-10)s_{k+1} - (N+2k+3)s_{k+2}]/(N-2k-1)$; |

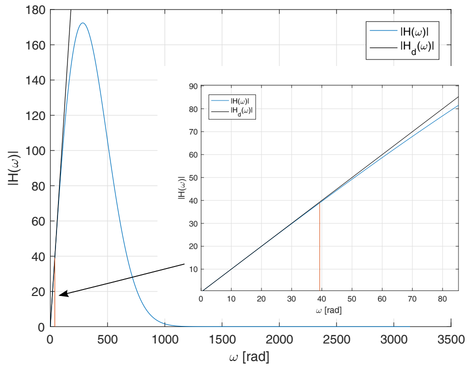


Figure 2. Frequency response of the first derivative noise-robust filter with setting $N = 51$, $h = 0.001[s]$.

system of linear equations

$$Y = W\theta + \rho, \tag{20}$$

where $Y$ is $pn$-vector, $p$ denotes the number of sampling points, $W$ is $pn \times (r-1)$ regression matrix, $\theta$ is $(r-1)$-vector of unknown parameters and $\rho$ is a vector of errors. The ordinary least squares (OLS) solution of (20) minimizes the 2-norm $\|\rho\|^2$ of the vector of errors $\rho$. The unicity of the estimation $\hat{\theta}$ depends on the rank of the matrix $W$. The numerical rank deficiency of $W$ can come from two origins: - structural rank deficiency which stands for any samples of $(q, \dot{q}, \ddot{q}, u)$ in $W$, - data rank deficiency due to a bad choice of noisy samples of $(q, \dot{q}, \ddot{q}, u)$ in $W$. This is the problem of the optimal excitation of the pendulum by the cart motion.

The regression matrix $W$ and vector $Y$ are perturbed by noise (from measurement and numerical differentiation) and by error modeling. Recall the effect of perturbation on the OLS solution of (20). Let $\hat{\theta} + \delta\hat{\theta}$ be the OLS solution of the perturbed system

$$Y + \delta Y = (W + \delta W)\theta + \rho \tag{21}$$

It can be shown that

$$\frac{\|\delta\hat{\theta}\|}{\|\hat{\theta}\|} \leq \mathrm{Cond}(W)\frac{\|\delta Y\|}{\|Y\|}, \text{ with } \delta W = 0,$$

$$\frac{\|\delta\hat{\theta}\|}{\|\hat{\theta} + \delta\hat{\theta}\|} \leq \mathrm{Cond}(W)\frac{\|\delta W\|}{\|W\|}, \text{ with } \delta Y = 0.$$

From it follows that the condition number $\mathrm{Cond}(W)$ is a quantity that measures the sensitivity of the solution $\hat{\theta}$ to errors in $W$ and $Y$. Moreover, if it is considered that $W$ is deterministic, and $\rho$ is a zero mean additive independent Gaussian noise, with standard deviation $\sigma_\rho$ such that

$$C_\rho = E(\rho\rho^T) = \sigma_\rho^2 I, \tag{22}$$

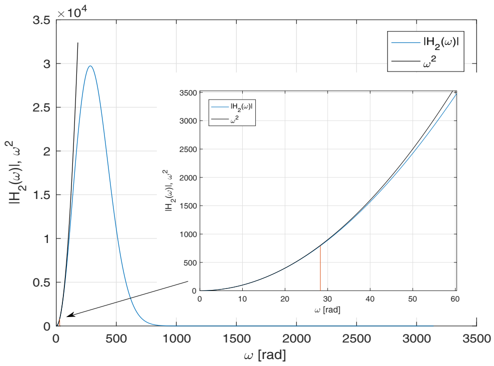


Figure 3. Frequency response of the second derivative noise-robust filter with setting $N = 101$, $h = 0.001[s]$.

where $E$ is the expectation operator and $I$ is the $pn \times pn$ identity matrix. Then an unbiased estimation of $\sigma_\rho$ can be

$$\sigma_\rho^2 = \frac{\|Y - W\hat{\theta}\|^2}{(pn - (r-1))}. \tag{23}$$

Further, the covariance matrix of the estimation error is given by

$$C_\rho = E[(\theta - \hat{\theta})(\theta - \hat{\theta})^T] = \sigma_\rho^2 (W^T W)^{-1}. \tag{24}$$

Thus, the standard deviation $\sigma_{\hat{\theta}_i}$ and its relative value $\sigma_{\hat{\theta}_{ir}}[\%]$, $i = 1, \ldots, r-1$ can be calculated by

$$\sigma_{\hat{\theta}_i} = \sqrt{C_{\hat{\theta}_i}(i,i)}, \qquad \sigma_{\hat{\theta}_{ir}} = 100\frac{\sigma_{\hat{\theta}_i}}{|\hat{\theta}_i|}.$$

The relative standard deviation can be used as a criterion to measure the quality of the identification value for each parameter. For example, if relative standard deviation of a parameter is greater than ten times the minimum relative standard deviation value, this parameter can be considered as poorly identified.

If the Lagrange equation (9) of joint $i, i = 1, \ldots, n$ is weighted with the inverse of standard deviation of the error calculated using the equations of joint $i$, then this weighting operation normalizes the errors and the weighted least squares (WLS) estimation of $\theta$ is obtained.

## IV. Experimental results on the triple inverted pendulum on a cart

We have tested the presented identification method on the real triple inverted pendulum. The experimental data was obtained from the free motion of the triple pendulum with the fixed cart. The experimentally measured angles of each pendulum joints was processed by (16) and (19) the position, velocity, acceleration data were used to create the regression model (20). The standard dynamic parameters was determined by the OLS and WLS method. According to Tab. II, the set of the standard dynamic parameters for the case $n = 3$, provides two exceptional parameters: $\frac{l_1}{l_2}$ and $\frac{1}{l_2}$, which can be obtained directly by measuring the lengths of the links. These parameters can be therefore used for checking of two identified values. The results are shown in the Tab. II and III. The free motion of the identified model and the real system with the fixed cart for the same initial conditions are compared in the Fig. 4 and Fig. 5.

Table II
STANDARD DYNAMIC PARAMETERS CALCULATED BY OLS AND WLS - CALCULATION OF THE WHOLE VECTOR $\theta$.

| St. dyn. parameter | OLS | $\sigma^{OLS}_{\hat{\theta}_i r}$ | WLS | $\sigma^{WLS}_{\hat{\theta}_i}$ |
|---|---|---|---|---|
| $\theta_1 = \frac{\mu_{12}}{\mu_{23}}$ | 5.4009 | 0.0807 | 5.4765 | 0.0777 |
| $\theta_2 = \frac{\mu_{13}}{\mu_{23}}$ | 0.7530 | 0.1172 | 0.7760 | 0.0642 |
| $\theta_3 = \frac{\kappa_1}{\mu_{23}}$ | 7.5698 | 0.0886 | 7.6796 | 0.0882 |
| $\theta_4 = \frac{\kappa_2}{\mu_{23}}$ | 6.3272 | 0.0671 | 6.3900 | 0.0682 |
| $\theta_5 = \frac{\kappa_3}{\mu_{23}}$ | 0.6088 | 0.3377 | 0.6049 | 0.0772 |
| $\theta_6 = \frac{\nu_1}{\mu_{23}}$ | 31.2593 | 0.1221 | 31.7122 | 0.1347 |
| $\theta_7 = \frac{\nu_2}{\mu_{23}}$ | 21.8344 | 0.1109 | 22.0310 | 0.1230 |
| $\theta_8 = \frac{\nu_3}{\mu_{23}}$ | 3.1453 | 0.5291 | 3.1193 | 0.1206 |
| $\theta_9 = \frac{b_1}{\mu_{23}}$ | 0.0540 | 50.4794 | 0.0580 | 56.9667 |
| $\theta_{10} = \frac{b_2}{\mu_{23}}$ | 0.0685 | 17.8808 | 0.0603 | 23.5155 |
| $\theta_{11} = \frac{b_3}{\mu_{23}}$ | 0.0329 | 17.9165 | 0.0569 | 3.1533 |

Table III
STANDARD DYNAMIC PARAMETERS CALCULATED BY OLS AND WLS - CALCULATION WITHOUT FRICTION PARAMETERS AND WITH KNOWN LENGTHS OF LINKS $l_1 = 0.25\,m$, $l_2 = 0.32\,m$.

| St. dyn. parameter | OLS | $\sigma^{OLS}_{\hat{\theta}_i r}$ | WLS | $\sigma^{WLS}_{\hat{\theta}_i}$ |
|---|---|---|---|---|
| $\theta_1 = \frac{\mu_{12}}{\mu_{23}}$ | 5.4890 | 0.0619 | 5.4924 | 0.0744 |
| $\theta_2 = \frac{\kappa_1}{\mu_{23}}$ | 7.6981 | 0.0702 | 7.7026 | 0.0858 |
| $\theta_3 = \frac{\kappa_2}{\mu_{23}}$ | 6.4006 | 0.0562 | 6.4034 | 0.0665 |
| $\theta_5 = \frac{\kappa_3}{\mu_{23}}$ | 0.6048 | 0.2596 | 0.6048 | 0.0561 |
| $\theta_6 = \frac{\nu_1}{\mu_{23}}$ | 31.7838 | 0.1089 | 31.8026 | 0.1364 |
| $\theta_7 = \frac{\nu_2}{\mu_{23}}$ | 22.0540 | 0.1058 | 22.0625 | 0.1227 |

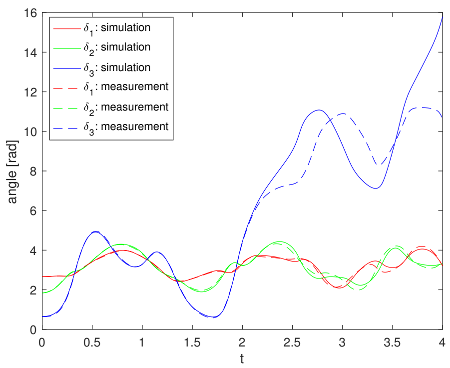

Figure 4. Comparison of the responses of the real system and identified model for initial conditions $\delta_{10} = 2.6605$ rad, $\delta_{20} = 1.8449$ rad, $\delta_{30} = 0.6459$ rad.

## V. CONCLUSION

The presented work deals with the problem of identification of the nLIP based on input/output behavior. Firstly, the mathematical model of the nLIP is formulated in the form of the nonlinear ordinary equations, where the cart acceleration is considered as the input and the angles of revolute joints as outputs of the system. Then, this model is reformulated

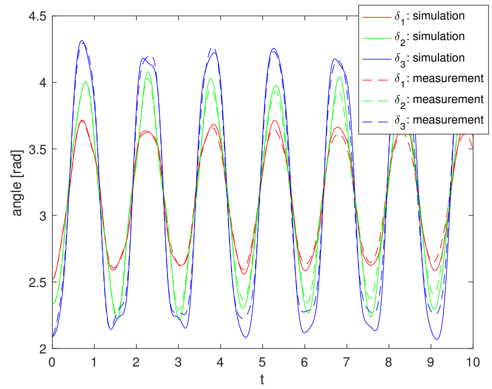

Figure 5. Comparison of the responses of the real system and identified model for initial conditions $\delta_{10} = 2.5218$ rad, $\delta_{20} = 2.3321$ rad, $\delta_{30} = 2.0890$ rad.

to the form which is linear with respect to some parameters - called standard dynamic parameters. Further, the explicit formulas for the standard dynamic parameters and explicit formula for the total number of them are provided for the general case. By a time equidistant sampling of the dynamical model with the standard dynamic parameters along some suitable trajectory, we obtain the overdetermined system of linear equations from which these parameters can be estimated by the ordinary or weighted least squares methods. Thus, the identification procedure provides the complete identification of all parameters needed to model the nLIP only on the measured signals. To the best of authors' knowledge, this is the first contribution so far providing the theoretical results for general case and experimental validation of the method for a real triple inverted pendulum.

## ACKNOWLEDGMENT


This paper was supported by Technology Agency of the Czech Republic from the project CIDAM TE02000103 and the project LO1506 of the Czech Ministry of Education, Youth and Sports under the program NPU I. The support is gratefully acknowledged.


## REFERENCES


[1] T. Glück, A. Eder, and A. Kugi, "Swing-up control of a triple pendulum on a cart with experimental validation," *Automatica*, vol. 49, no. 3, pp. 801–808, 2013.

[2] K. Graichen, M. Treuer, and M. Zeitz, "Swing-up of the double pendulum on a cart by feedforward and feedback control with experimental validation," *Automatica*, vol. 43, no. 1, pp. 63–71, 2007.

[3] S. Jadlovský and J. Sarnovský, "Modelling of classical and rotary inverted pendulum systems–a generalized approach," *Journal of Electrical Engineering*, vol. 64, no. 1, pp. 12–19, 2013.

[4] L. Zhang and Y. Tu, "Research of car inverted pendulum model based on lagrange equation," in *Intelligent Control and Automation, 2006. WCICA 2006. The Sixth World Congress on*, vol. 1, pp. 820–824, IEEE, 2006.

[5] W. Khalil and E. Dombre, *Modeling, identification and control of robots*. Butterworth-Heinemann, 2004.

[6] R. Čečil, V. Šetka, and M. Schlegel, "Radio module for fast real-time control of inverse triple pendulum," in *Wireless Systems within the Conferences on Intelligent Data Acquisition and Advanced Computing Systems (IDAACS-SWS), 2016 3rd International Symposium on*, pp. 80–84, IEEE, 2016.

[7] P. Holoborodko, "Smooth noise robust differentiators." http://www.holoborodko.com/pavel/numerical-methods/numerical-derivative/smooth-low-noise-differentiators/.